Contribution from the Departments of Chemistry, Princeton University, Princeton, New Jersey 08544, and University of Maine, Orono, Maine 04473

One- and Two-Photon Spectroscopy of the Hexafluoroplatinate(IV) Ion

Cecelia Campochiaro,[§] Donald S. McClure,*[,†] and Howard H. Patterson[‡]

Received November 19, 1991

One- and two-photon excitation spectra of Pt^{IV} in Cs_2MF_6 (M = Si, Ge) were taken at high resolution and low temperatures using laser methods. The zero-phonon line of the first absorption and emission transition was found to be located at 19 490 ± 15 cm^{-1}, although it has not been directly observed. A zero-phonon line of the $^1A_{1g} \rightarrow {}^3T_{1g}(A_{1g})$ multiplet component was identified at 27 030 cm^{-1}, and it permitted us to reassign the one-photon spectrum of Patterson from 27 000 to 30 000 cm^{-1}. The $\nu_4 t_{1u}$ mode is active in promoting the $^1A_g \rightarrow {}^3T_{1g}(A_{1g})$ transition as well as the fluorescence and absorption between $^1A_{1g}$ and $^3T_{1g}(E_g)$. The ν_3 mode is active only in the latter transition and ν_6 was not observable. Bond length changes upon excitation to several excited states were determined. A standard crystal field calculation gave an accurate account of the energy level positions determined in this work.

Introduction

For the heavy transition elements, the d^6 configuration in octahedral coordination represents a stable closed shell, t_{2g}^6. The first electronic transition in the d-shell is $t_{2g}^6 \rightarrow t_{2g}^5 e_g$, giving rise to the four terms $^3T_{1g}$, $^3T_{2g}$, $^1T_{1g}$, and $^1T_{2g}$ in order of increasing energy. Because of the replacement of a t-orbital by an e-orbital in this set of transitions there is a large Franck–Condon displacement, and there are probably Jahn–Teller distortions as well. The absorption and emission bands are, therefore, broad, though sometimes structured. In this paper the spectra of Pt^{4+} in Cs_2GeF_6 and Cs_2SiF_6 are studied by one- and two-photon spectroscopy in order to locate or estimate the positions of the zero-phonon lines and to learn more about the details of excited state distortions. In a related paper Rh^{3+} in several elpasolite host crystals was studied.[1]

The tetravalent ions in the antifluorite type host crystals such as Cs_2GeF_6 have been studied extensively. For example, Mn^{4+} has been studied by Flint et al.,[2] by Manson et al.,[3] and in this laboratory.[4] The group of H. Patterson has published on Pt^{4+}.[5-7] Our work is an extension of this.

Figure 1 is an energy level diagram of Pt^{4+} in an octahedral field resulting from a crystal field calculation using the parameters listed in the caption.[6] The experimental results show that this diagram gives a reasonably good approximation to the peaks of the electronic bands. Thus the emission spectrum is due to $^3T_1(E) \rightarrow {}^1A_1$. (Hereafter the "g" subscript will be omitted from the electronic state symbols.) It is highly efficient, and served as a means for detecting one- and two-photon excitation. The large spin–orbit coupling evident in the diagram is consistent with the approach to *j–j* coupling in the atom. The low-energy group of levels E, T_2, and T_1 from $^3T_1$, seen in Figure 1, can be described by coupling the lower of the t_2-hole spin orbitals having e″ (or Γ_7) symmetry to the e-electron spin orbital having U (or Γ_8) symmetry.

The two-photon selection rules show that the lowest observable transitions and polarizations are $^1A_1 \rightarrow {}^3T_1(E)$ $(1 - {}^3/_4 \sin^2 2\theta)$, $^3T_1(T_2)$ $(\sin^2 2\theta)$, $^3T_1(A_1)$ (isotropic), and $^3T_1(T_1)$ (forbidden), with similar results for $^3T_2$ (but $^1A_1 \rightarrow A_2$, T_1 (forbidden)).[8] The $^1A_1 \rightarrow {}^1T_1$ transition is forbidden, but may appear vibronically, and the $^1A_1 \rightarrow {}^1T_2$ transition should be allowed $(\sin^2 2\theta)$. Here, θ is the angle between the 100 axis and the polarization vector when the light propagates along 001.

Superimposed on these polarization rules is the fact that transitions $t_2 \rightarrow e$ should be polarized as $\sin^2 2\theta$, having a maximum at 45° to a ⟨100⟩ axis. In the presence of the large spin–orbit coupling, the one-electron configurations are mixed, and this selection rule is degraded. We did not observe significant polarizations. The detailed explanation of this result is considered later.

Even without the polarizations, the two-photon spectra gave valuable new information leading to a reassignment of the spectrum of Pt^{4+}.

An important goal of the present work is to understand the gap between fluorescence and absorption. In the previous work the gap was about 3000 cm^{-1}.[6] In actuality there must be no gap, and a zero-phonon line must exist appearing in both absorption and emission. In the present case the transition is $^1A_1 \rightarrow {}^3T_1(E)$ and only an electric quadrupole operator of E-symmetry can cause a one-photon transition., A two-photon transition having an operator with the same symmetry should be allowed. In actual fact, a one-photon excitation spectrum coupled with the emission spectrum provided the most information about the location of the zero-phonon line.

Experimental Section

The Cs_2SiF_6:Pt 1% mixed crystals were made by first synthesizing Cs_2PtF_6 by fluorinating Cs_2PtCl_6 with BrF_3.[9] The host crystals were made by adding CsF to 30% aqueous H_2SiF_6 and filtering the resulting precipitate on acid-washed filter paper. The correct proportions of host and guest were dissolved in 48% aqueous HF to make a nearly saturated solution. The solution was kept in a polypropylene beaker and enclosed with KOH pellets in a sealed polypropylene bag for several days until crystals formed. Most of the crystals grew as hexagonal plates, but we used the few cubes which formed. These were polished with 0.3-μm alumina grit suspended in water. Cs_2SiF_6:Pt, Cs_2GeF_6:Pt, and Cs_2PtF_6 crystals from a previous investigation were also used. The new Cs_2SiF_6:Pt crystals exhibited spectra identical to the older ones.

All of the spectra shown in this paper were taken at temperatures of 5–10 K using either a Janis Super Varitemp dewar or a closed-cycle helium refrigerator.

The two-photon spectrometer consisted of a Quantel YG-580 instrument with amplifier operating at 10 Hz pumping the oscillator and preamplifier of a Lambda Physik FL3002 dye laser. The dye laser was focussed onto the crystal to reach a power density of about one GW/cm^2 and backed off to prevent breakdown.

The fluorescence was collected by a *f*/3 condenser and passed through the leaves of a Uniblitz shutter to another *f*/3 condenser and to a cooled GaAs photomultiplier tube. The shutter would open approximately 1 ms after the laser fired and stay open for several milliseconds. The Pt^{4+} emission has a half life of 7.5 ms. Photon-counting electronics was used for the two-photon experiments. The background was less than three counts within a 7-ms gate, and the weakest features recorded 10–30 counts. The one-photon excitation spectra were many orders of magnitude stronger. The background in the one-photon experiment was

† Princeton University.
‡ University of Maine.
§ Present address: Department of Chemistry, Stanford University, Stanford, CA 94305.

(1) Weaver, S. C.; McClure, D. S. *Inorg. Chem.*, following paper in this issue.
(2) Manson, N. B.; Shah, G. A.; Howes, B.; Flint, C. D. *Mol. Phys.* **1977**, *34*, 1157.
(3) Hasan, Z.; Manson, N. B. *J. Phys. C* **1980**, *13*, 2325.
(4) Chien, R.-L.; Berg, J. M.; McClure, D. S.; Rabinowitz, P.; Perry, B. *J. Chem. Phys.* **1986**, *84*, 4168.
(5) Laurent, M. R.; Patterson, H. H.; Pike, W.; Engstrom, H. *Inorg. Chem.* **1981**, *20*, 372.
(6) Patterson, H. H.; DeBerry, W. J.; Byrne, J. E.; Hsu, M. T.; LoMenzo, J. A. *Inorg. Chem.* **1977**, *16*, 1698.
(7) Patterson, H. H.; Lynn, J. W. *Phys. Rev.* **1979**, *B19*, 1213.
(8) Bader, T. R.; Gold, A. *Phys. Rev.* **1989**, *71*, 99.
(9) Dixon, K. R.; Sharp, D. W.; Sharpe, W. A. *Inorg. Synth.* **1970**, *12*, 232.

0020-1669/92/1331-2809$03.00/0

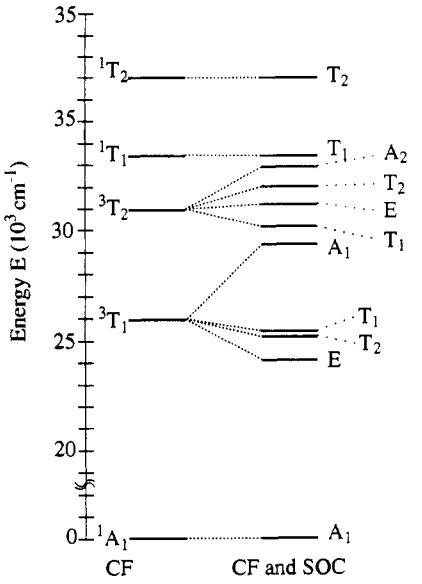

Figure 1. Energies and labels of the ground t_2^6 and excited t_2^5e states of the PtF_6^{2-} anion. The splittings are the result of a crystal field (CF) calculation fitted to the OP spectrum in ref 6. The left side of the diagram presents the states in the absence of spin-orbit coupling (SOC). Dq = 3150 cm^{-1}, ζ = 3579 cm^{-1}, B = 395 cm^{-1}, and C = 2254 cm^{-1}.

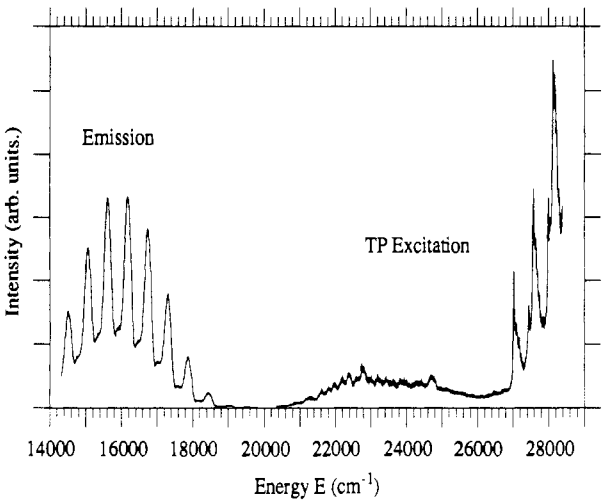

Figure 2. Emission and two-photon excitation spectrum of Cs_2GeF_6:Pt^{4+} taken at 10 K.

several hundred counts due to amplified spontaneous emission, but the weakest signals reported were about 100 counts above the background.

Results

A. Emission Spectrum. The emission spectrum has been studied extensively by others.[5,7] The left side of Figure 2 shows the emission of Pt^{4+} in Cs_2GeF_6 as host crystal; the spectrum when Cs_2SiF_6 is used is nearly identical. The right side of Figure 2 shows the two-photon spectrum, which will be discussed later. We have calibrated the emission spectrum very carefully using a Ne pen lamp and fitted the vibrational progression to a standard anharmonic oscillator formula, as did Laurent et al.[5]

$$E(v) = wv - xv^2 \quad (1)$$

with w = 581 cm^{-1} and x = 2 cm^{-1}, fitting the observed intervals to a mean deviation of 2 cm^{-1}, within the error limits of the previous work.

Figure 2 shows the first observed emission feature to be at 19040 cm^{-1}. If there is another feature at a higher frequency, it is within the noise level as it is not observed. It would, therefore, have to be about a factor of 10 weaker than the 19040-cm^{-1} band. The 19040 cm^{-1} is not likely to be the electronic origin since its spacing relative to the other bands fits into the progression. The

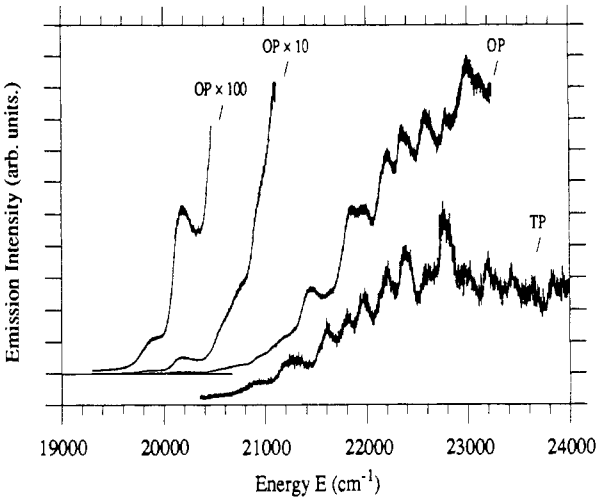

Figure 3. One- and two-photon spectra of Cs_2GeF_6:Pt^{4+}. The OP spectrum is enlarged between 19000 and 21000 cm^{-1} so the weak features near the origin estimated to be at 19500 cm^{-1} can be revealed.

electronic origin is likely to be spaced by a non totally symmetric vibrational frequency above 19040 cm^{-1}. The available frequencies are those of the odd parity modes in the ground state. The modes of PtF_6^{2-} are as follows: a_{1g}, ν_1, 591; e_g, ν_2, 573; t_{1u}, ν_3, 571; t_{1u}, ν_4, 281; t_{2g}, ν_5, 218; t_{2u}, ν_6, 152.[5,6] Both ν_3 and especially ν_4 are active in promoting fluorescence progressions according to ref 5.

The frequency of 581 cm^{-1} in the emission spectrum is not one of the normal mode frequencies, but is nearly the average of 591 a_g and 573 e_g. Patterson has interpreted this result to mean that there is a large Jahn–Teller displacement in the e_g mode in the excited state.[5]

Zink and Reber[10] have analyzed this type of progression in K_2PtF_6.

The intensity distribution in the emission spectrum can be fitted approximately to a Poisson distribution with S = 6 when the ν^3 factor for the radiation rate is included.

Another feature of the emission spectrum is the evidence for a weaker progression in a mode of ~580 cm^{-1} beginning at about 18780 cm^{-1}.

B. The $3T_1$ Multiplet. In marked contrast to the apparent simplicity of the emission spectrum is the first absorption region from about 20000 to 27000 cm^{-1} seen in Figure 2 as a two-photon spectrum. Three of the components of $^3T_1$, namely, E, T_1, and T_2, should lie in this range. The total degeneracy of 8 along with Jahn–Teller forces could easily be responsible for the complexity observed here. The distinct and sharp progression starting at 27000 cm^{-1} will be assigned to the $^3T_1(A_1)$ state. The relative isolation and nondegeneracy of this state may account for the simplicity of its spectrum compared to that of the region of the E, T_1, and T_2 states.

The two-photon spectrum from 20000 to 27000 cm^{-1} was weak and could not be detected with adequate signal/noise ratio at energies below 20500 cm^{-1} as seen in Figure 2. Figure 3 shows the one-photon excitation spectrum compared to the two-photon spectrum. By the use of pulsed laser excitation, the one-photon spectrum can be detected with good signal/noise down to 19300 cm^{-1}.

Figure 4 shows the beginning of emission and of the one-photon excitation together. In ref 6 the absorption spectrum appears to begin at 22000 cm^{-1}, nearly 3000 cm^{-1} above the first emission feature at 19040 cm^{-1}. Figure 4 shows a weak broad feature at 19860, only 824 cm^{-1} above the first emission band. From figure 3 it can be estimated that the 19860-cm^{-1} band is 750 times weaker than the 23000 cm^{-1} band, the most prominent band in the one-photon excitation spectrum. This is in contrast to the first emission band whose intensity relative to the stronger fluorescence band is $^1/_{80}$.

(10) Zink, J.; Reber, C. *Coord. Chem. Rev.* **1991**, *111*, 1–14.

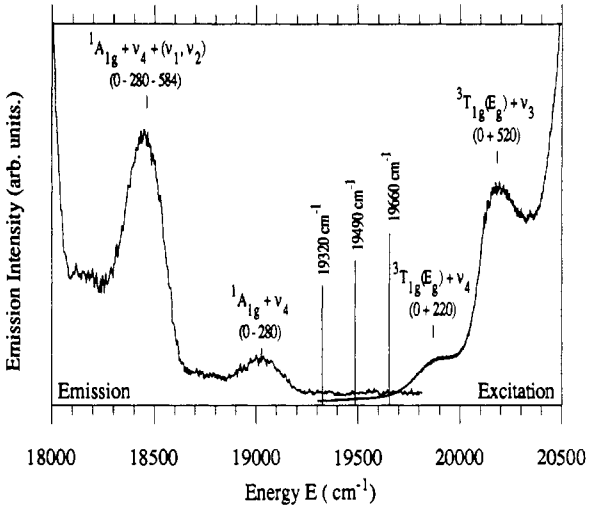

Figure 4. Emission and excitation spectra of $Cs_2GeF_6:Pt^{4+}$ near the zero phonon origin. The placement of the lines at 19 320, 19 490, and 19 660 cm^{-1} are discussed in the text.

Figure 4 shows that the band widths are about the same in excitation and emission, 150 cm^{-1}. It seems likely that the widths represent excitation of lattice modes rather than an effect of inhomogeneous broadening (see Discussion). The bandwidth would then represent the Franck–Condon distribution of the lattice modes required to map the excited- and ground-state lattice geometries onto each other. Most of the intensity of the zero-phonon "line" would then be distributed into these modes, making it much less detectable.

It is only a short additional step now to locate the 0–0 line. The enabling modes in the emission must be $\nu_4(281)$, $\nu_3(571)$, or $\nu_6(152)$. If 19 040 cm^{-1} is the first member of the strong series in emission induced by a low-frequency mode and 18 750 cm^{-1} is the first member of the weak series, the difference of 290 cm^{-1} is the same as the difference between ν_3 and ν_4, 571 − 280 = 291 cm^{-1}. Thus, the peak of the lattice emission band corresponding to the 0–0 line would be at 19 040 + 280 = 19320 cm^{-1} as shown in ref 6. Assuming that the band shape of the unobservable 0–0 band is the same as that of the 19 040-cm^{-1} band we then add the peak to origin energy of that band to 19 320 cm^{-1} to obtain 19 320 + 170 = 19 490 cm^{-1} with an uncertainty of about 15 cm^{-1}. This should be the position of the unobserved 0–0 line.

In order to analyze spectra we must use the peaks rather than the origins of the lattice bands since they are more observable. Therefore the emission spectrum is analyzed using 19 320 cm^{-1} as the origin and the absorption or excitation spectra are analyzed using 19 490 + 170 = 19 660 cm^{-1} as the origin. Having established these origins, we now present the "line" lists for the spectra in Tables I and II, which give the positions of the observed peaks and analyses based on the estimated origin peaks.

Table I fills in the section of Table II in ref 6 from 23 440 to 19 660 cm^{-1} which was missing from this work due to the lower sensitivity of the photographic measurement. The two columns labelled OI(220) and OII(520) give the frequency differences from the first two bands 19 880 cm^{-1}, 220 cm^{-1} from the origin, and 20 180 cm^{-1}, 520 cm^{-1} from the origin. These are considered to be the vibronic origins. From their frequency values 220 and 520 are likely to be ν'_4 and ν'_3, respectively. Our Table II gives as much of the early part of the two-photon spectrum as we could measure, with ΔE being the frequency relative to the absorption origin 19 660 cm^{-1}. Tables I and II, therefore, list the observable "lines" up to 3200 cm^{-1} from the true origin. The line widths and intensities are also shown. The widths are from 50 to 150 cm^{-1} so that frequency intervals cannot be given with great accuracy.

Figure 3 also compares the one- and two-photon spectra, and it is clear that there are some similarities. The best way to compare them is to superpose one on the other with a relative shift of the OP spectrum to the red to subtract out the frequency of the enabling vibration. At present, the TP spectrum up to 27 000 cm^{-1} is incomplete and noisy. But if the relative shift is about 520 cm^{-1}, the two spectra seem nearly to coincide up to 22 400 cm^{-1} in the TP spectrum. There is almost as good a correspondence when the relative shift is 220 cm^{-1}. Our one-photon excitation spectrum is also incomplete, but using data of ref 6 the coincidences are extended to 23 000 cm^{-1} in the TP spectrum when the OP is red shifted by 520 cm^{-1}.

Even with these aids to an analysis of this spectral region we cannot be confident of a true assignment. The problem is that the T_2 multiplet component could begin as low as 20 500 cm^{-1} and contribute relatively strong vibrational lines by 21 500 cm^{-1}. In fact, the character of the two-photon spectrum changes from one having broad bands (~150 cm^{-1}) to narrower ones at about 21 600 cm^{-1}. If polarized two-beam, two-color spectra can be obtained, the E absorption could be eliminated and the distinction between the spectra of the E and T_2 components could be made.

Table I. Energies of the Features Observed via One-Photon Excitation of $Cs_2GeF_6:Pt^{4+}$ in the Region of the $^3T_{1g}$ (E_g, T_{2g}, and T_{1g}) States[a] Where 19 660 cm^{-1} Is the Origin

line	energy (vac), cm^{-1}	ΔE, cm^{-1}		fwhm, cm^{-1}	rel intens
	19 880	OI (220)		135	0.0004
	20 180		OII (520)	160	0.0017
	20 580	700	400	140	0.0054
	20 740	860	560	140	0.0089
	20 915	1035	735	80	0.017
	21 160	1280	980	90	0.037
	21 440	1560	1260	135	0.088
	21 635	1755	1455	?	0.085
	21 850	1970	1670	145	0.17
	21 970	2090	1790	110	0.17
3-0	22 210	2330	2030	110	0.23
	22 350	2470	2170	65	0.25
3-A	22 400	2520	2220	65	0.25
3-B	22 585	2705	2405	120	0.27
	22 725	2845	2545	?	0.24
3-C	22 780	2900	2600	50	0.27
3-D	23 000	3120	2820	100	0.33

[a] The line designation on the left is from Table II in ref 6. Another line designated 3-0 at 22 210 cm^{-1} has been read off Figure 3 in ref 6. Except for line 3-A, which is broad, our five measurements in the region where we overlap agree within 10 cm^{-1}, which is approximately the accuracy with which these features can be read.

Table II. Energies of the Features Observed via Two-Photon Excitation of $Cs_2GeF_6:Pt^{4+}$ in the Region of the $^3T_{1g}$ (E_g, T_{2g}, and T_{1g}) States Where 19 660 cm^{-1} Is the Origin

energy (vac), cm^{-1}	ΔE, cm^{-1}	fwhm, cm^{-1}	rel intens
20 900	1240	150	0.024
21 300	1640	110	0.048
21 600	1940	100	0.084
21 800	2140	90	0.093
21 970	2310	100	0.14
22 210	2550	100	0.14
22 400	2740	70	0.16
22 650	2990	90	0.14
22 790	3130	80	0.17

C. Higher States. The two-photon spectrum from 27 000 to 30 000 cm^{-1} has a much simpler appearance than the previous band, as seen in Figures 2, 5, and 6: it begins with a strong band at 27 030 cm^{-1} and continues with a progression in a symmetric mode of about 545 cm^{-1}. A lower frequency mode of 420 cm^{-1} is the origin of another progression in the 545-cm^{-1} mode. Figure 5 shows that this spectrum is nearly the same for the two host crystals used. The simplicity of this spectrum compared to the first region is consistent with our assignment of it to the A_1 component of $^3T_1$. Its vibrational analysis is given in Table III.

This table also shows the fit to the anharmonic oscillator formula of eq 1 with the parameters w = 549.4 and x = 4.2. The mean deviation of the spectral lines from this formula is 12 cm^{-1}.

The spectral peaks given in Table III do not have quite as simple an interpretation as implied by the vibrational analysis given for them there. In Figure 5, one can see that the lattice sideband

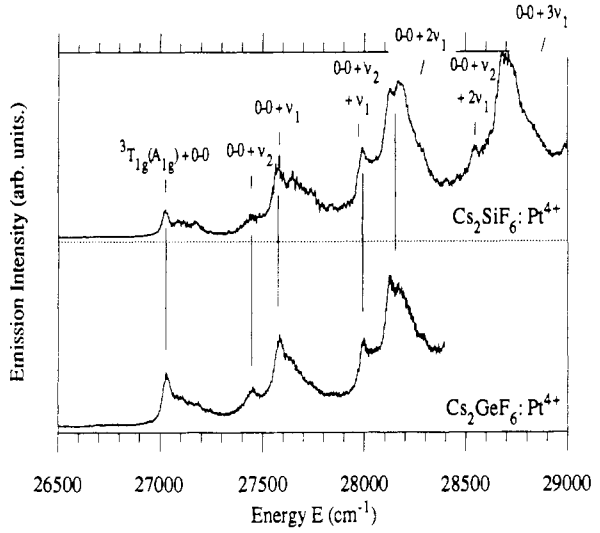

Figure 5. Detail of the $^1A_{1g} \rightarrow {}^3T_{1g}(A_{1g})$ transition observed via two-photon excitation of Cs_2GeF_6:Pt^{4+} and Cs_2SiF_6:Pt^{4+}.

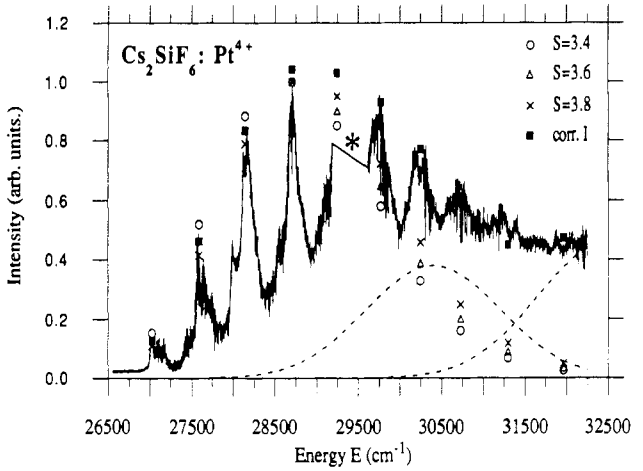

Figure 6. Plot of the $^1A_{1g} \rightarrow {}^3T_{1g}(A_{1g})$ transition observed via two-photon excitation of Cs_2SiF_6:Pt^{4+}. The asterisk denotes a region where we have no data. The best fit of a Poisson distribution to the first few peaks gives $S = 3.6$; this is shown graphically in the figure. The dashed lines represent two Gaussians added to the peak intensities given by $S = 3.6$, and the solid squares show the improved fit. The higher energy Gaussian band corresponds to the $^1T_{1g}$ state. The other Gaussian may correspond to the $3T_{2g}(E_g)$ and $^3T_{2g}(T_{2g})$ states.

of each peak gets stronger and narrower with increasing vibrational quantum number, and that its strength is greater for the Si lattice than for the Ge lattice. The intensity maximum of the third peak includes a strong lattice sideband, and the $(v = 1) - (v = 2)$ interval will be read as 40 cm^{-1} too high. Therefore the lattice sideband affects the shape of each progression member in a different way, and even affects the apparent center frequency.

Figure 6 shows the two-photon spectrum of Cs_2SiF_6:Pt from 27 000 to 31 700 (Due to an accident some data near 29300 cm^{-1} were lost.) The sharp features of this spectrum are the members of the a_{1g} progression in the $^3T_1(A_1)$ state. Additional two-photon absorption is evident at the higher end of this spectrum, however. The spectrum could be fitted with a Huang–Rhys factor of $S = 3.6$ for the first four bands as shown in this figure, but the intensity subsequently remains too high for such a distribution. From the energy level diagram of Figure 1 we expect that the $^3T_2$ and $^1T_1$ states will begin to contribute in this higher energy region. Figure 6 shows a pair of Gaussian distributions at the expected locations of these states which fit the observed intensity. The progression members attributable to $^3T_1(A_1)$ still seem to be identifiable out to 31185 cm^{-1} (8 ν_1) as shown in Table III where the bands of this series in the two-photon spectrum are listed. No additional fine structure is observed.

Table III. Energies and Assignments of the 27030-cm^{-1} Band in the Two-Photon Spectrum of Cs_2SiF_6:Pt^{4+} [a]

energy (vac), cm^{-1}	ΔE, cm^{-1}	assignts (0 = 27 030 cm^{-1})	ΔE(calc), cm^{-1}
27 030	0	$^3T_{1g}(A_{1g})$ 0–0	
27 105	75	L^{1+}, L^{2+}, and L^{3+} phonons	
27 175	155	L^{2+} phonon	
27 449	419	0–0 + ν_2	420
27 575	545	0–0 + ν_1	548.3
27 997	967	0–0 + ν_2 + ν_1	968
28 135	1105	0–0 + 2ν_1	1088
28 540	1510	0–0 + ν_2 + 2ν_1	1508
28 675	1645	0–0 + 3ν_1	1620
29 030	2000	0–0 + ν_2 + 3ν_1	2040
29 172 (est)		0–0 + 4ν_1	2142
29 592 (est)		0–0 + ν_2 + 4ν_1	2562
29 673	2643	0–0 + 5ν_1	2657
30 060	3030	0–0 + ν_2 + 5ν_1	3077
30 170	3140	0–0 + 6ν_1	3163
30 550	3520	0–0 + ν_2 + 6ν_1	3583
30 690	3660	0–0 + 7ν_1	3661
31 185	4155	0–0 + 8ν_1	4152

[a] The ΔE value resulting from the assignment is given at the right, where ν_2 = 420 cm^{-1} and the ν_1 progression is given by $\Delta E = 552.5v - 4.2v^2$. The estimates of line positions where data were lost at 4ν_1 were made from this formula.

The $^3T_2$ term splits into a lower T_1 level and three close levels E, T_2, and A_2. Both T_1 and A_2 are symmetry forbidden in the two-photon spectrum so that only the close pair E, T_2 would contribute.

The $^1T_1$ state is also symmetry forbidden in the two-photon spectrum so that only weak vibronic contributions are expected from it. Therefore, the analysis of the 28 500–32 500-cm^{-1} region shown in Figure 6 seems reasonable as the $^3T_1(A_1)$ state could have greater two-photon intensity than the nearby $^3T_2$ and $^1T_1$ states.

The one-photon spectrum of ref 6 shows the $^1T_1$ state with a clear progression in ν_1 (=540 cm^{-1}) having its maximum intensity at the 32 450-cm^{-1} band. The beginnings of the $^1T_2$ band are seen at 35 000 cm^{-1} in the one-photon spectrum. This region is still accessible to a two-photon study but has not been investigated as yet.

Discussion

The two-photon spectra have provided new information to help interpret the spectrum of PtF_6^{2-}. Our one-photon laser spectroscopy has also been important in solving the problem of the gap between emission and absorption.

In fact, there should never be a gap between emission and absorption as there must always be a vibrationless ground and a vibrationless excited state and a transition energy between them. The only question is: how weak is the zero phonon line? The present case of PtF_6^{2-} is an interesting one, intermediate between weak and strong coupling. An apparent gap of about 3000 cm^{-1} has been shown here to be a few hundred reciprocal centimeters by using the 500-fold increase in sensitivity provided by a pulsed laser in comparison to the photographic method used in ref 6.

The first emission band at 19 040 cm^{-1} and the first excitation band at 19 880 cm^{-1} are each of the same width, about 150 cm^{-1}. When they are assigned as in the previous section, their identification appears reasonable. The zero phonon "bands" peaking at 19 660 and 19 320 cm^{-1} in absorption and emission cannot overlap if this assignment is accepted, and therefore their width does not arise from inhomogeneous broadening. This width is presumed to represent a "Franck–Condon distribution" of lattice vibrations peaking at about 150 cm^{-1} and extending to over 300 cm^{-1}. According to Patterson and Lynn,[7] a group of acoustic and low-frequency optical modes in Cs_2SiF_6 extend up to 140 cm^{-1}, with the internal modes of the octahedron beginning only at 239 cm^{-1} when ν_6 is excited. Thus, the continuous 300-cm^{-1} distribution must represent multiple excitations of the 0–140-cm^{-1} modes. The coupling of PtF_6^{2-} to the Cs_2SiF_6 lattice must therefore be much stronger than that of MnF_6^{2-}. With even stronger coupling, the

Table IV. Reassignment of the One-Photon Spectrum Beginning at 27 030 cm^{-1}, with the Lines Designated as in Ref 6[a]

name	energy (vac), cm^{-1}	ΔE	assigns	ΔE(calc), cm^{-1}
zero-phonon	27 030	0	zero-phonon line from two-photon spectrum	
3-X	27 090	60	lattice mode	
3-Y	27 250	220	ν_4	220
4-A	27 650	620	$\nu_4 + \nu_2$	640
4-B	27 790	760	$\nu_4 + \nu_1$	765
	27 950	920		
4-C	28 210	1180	$\nu_4 + \nu_2 + \nu_1$	1185
4-D	28 320	1290	$\nu_4 + 2\nu_1$	1270
	28 500			
4-F	28 760	1730	$\nu_4 + \nu_2 + 2\nu_1$	1730
4-G	28 890	1860	$\nu_4 + 3\nu_1$	1865
4-H	29 060			
4-I	29 300	2270	$\nu_4 + \nu_2 + 3\nu_1$	2275
4-J	29 420	2390	$\nu_4 + 4\nu_1$	2400
4-K	29 600	2580		
5A	29 850	2820	$(\nu_4 + 4\nu_1 = 2820)$	$^1T_1$ origin
5B	29 960	2930	$(\nu_4 + 5\nu_1 = 2945)$	$^1T_1$ origin

[a] The line designations and the line frequencies are from Table II in ref 6. ΔE is measured from 27 030 cm^{-1}. The assignment and the resulting ΔE value given on the right are based on the nominal frequencies ν_1 = 545 cm^{-1}, ν_2 = 420 cm^{-1}, and ν_4 = 220 cm^{-1}.

space between the molecular modes would fill in and a broad continuum would be observed as is typical of many solid-state spectra.

The, so far, unobserved origin is a zero-phonon line at about 19 490 cm^{-1} with a Frank–Condon distribution of lattice modes to the blue in absorption and to the red in emission. The two-photon transition to this phonon sideband and the zero phonon line are symmetry allowed and may be observable in a more sensitive experiment.

The two-photon results permit a reinterpretation of the one-photon spectrum between 27 000 and 30 000 cm^{-1}. The zero-phonon line of the $^3T_1(A_1)$ state at 27 030 cm^{-1} serves as the origin of the spectrum of Figure 4 in ref 6, as shown in Table IV. In Table IV we have copied the line list of ref 6 using the original notation but making the new assignments. The line $3 - y$ at 27 250 cm^{-1} is now seen to be the false origin at 220 cm^{-1}, undoubtedly ν_4, as it has the same frequency as in the $^3T_1(E)$ state. As in the two-photon spectrum, there is a progression in ν_1, about 545 cm^{-1}, and another progression starting on the false origin plus ν_2 = 400 cm^{-1}, denoted as line 4-A at 27 650 cm^{-1}. The progression of doublets is caused by the difference between ν_2 and ν_1 just as in the two-photon spectrum.

In making the one- and two-photon correlation we have to take account of the possible errors and inaccuracies of both measurements. The value of 400 cm^{-1} for ν_2 found above from the one-photon spectrum does not agree exactly with the value 420 cm^{-1} found from the two-photon spectrum. The latter is more likely to be correct since it comes from a single data set, whereas the 400 cm^{-1} value is a result of comparing one- and two-photon data sets. In any case, the spectral "lines" are 50–100-cm^{-1} wide, so that a 20 cm^{-1} shift cannot easily be measured. A good analysis of the one-photon spectrum consistent with the two-photon spectrum can be made with ν_4 = 220 cm^{-1} and $\nu_4 + \nu_2$ = 220 + 420 cm^{-1} as false origins and ν_1 = 545 cm^{-1} forming progressions, the same frequencies as in the two-photon spectrum.

One interesting difference between the one- and two-photon spectra is that the one-photon progression built on 220 cm^{-1} is weaker than that built on 220 + 420 cm^{-1}, while the reverse is true for the two-photon progressions built on 0 and 0 + 420 cm^{-1}. The reason for ν_2 to appear at all in this spectrum is related to vibrational–electronic coupling, a remnant of the Jahn–Teller effect, and the relative intensity of ν_1 and ν_2 in the progression may be determined by anharmonic coupling. It would be worthwhile to get a photoelectric high-resolution one-photon spectrum of this region to record this phenomenon more accurately.

According to Table IV, lines 5A and 5B seem to be a part of the progression in the $^3T_1(A_1)$ state since they fit as accurately as the preceding members. The intensities do not fit, however, and we think these are the false origins of the $^1T_1$ progression, as assigned in ref 6. If so, then the $^1T_1$ origin would be at 29 850 − (220 + 420) = 29 210 cm^{-1} if ν_4 and ν_2 are the same as in $^3T_1(A_1)$.

The ν_4 mode is the major enabling mode of the $^3T_1(E) \rightarrow {}^1A_1$ emission and of the one-photon $^1A_1 \rightarrow {}^3T_1(A_1)$ absorption, but it was secondary to ν_3 in the $^1A_1 \rightarrow {}^3T_1(E)$ absorption. This is another point to be resolved in a detailed study of the vibronic coupling.

The lack of polarization of the two-photon bands may be caused by crystal defects. The crystals often showed regions of birefringence which should not have been present. We did not have an imaging system in place to determine the optimum spot for laser excitation of the crystal. Another possibility is that the crystals are being damaged by the laser. We can avoid pitting at the surface, which occurs at high power densities, but less drastic effects may cause depolarization.

If the $^3T_1(E)$ emission and the $^3T_1(A_1)$ and $^1T_1$ absorption are assumed to have a_{1g} progressions and that only the near-neighbor F^- ions are displaced in transitions to or from the ground state, then the bond length changes in the transitions may be estimated. These are −0.78, 0.62, and 0.80 Å for the above transitions.

Conclusion

The nature and location of the $^1A_1 \rightarrow {}^3T_1$ (E) zero-phonon line has been established. The odd parity modes which induce the one-photon absorption or emission appear to be ν_3 and ν_4 in each case, although they have different activities in emission and absorption. These modes may well change their character upon electronic excitation, which would explain this latter fact.

We have reassigned the components of the $^3T_1$ term, based on the particularly clear appearance of the two-photon A_1 spectrum. Previously, this region had been ascribed to the T_1 components of $^3T_1$.[6]

The major spectral features are well explained by a standard d^6 crystal field calculation including spin-orbit coupling. With the above reassignment, it appears that the E, T_2, and T_1 components of $^3T_1$ are indeed confined to the 19 500–27 000-cm^{-1} region while the A_1 component is well above the others, peaking at about 29 000 cm^{-1}. These are close to the positions given in Figure 1.

Acknowledgment. We appreciate the assistance of Mark Thompson in helping with the synthesis of Cs_2PtF_6 and Latonya Kilpatrick and Tom Spiro for the use of their Raman spectrometer for taking luminescence spectra. This research was funded by Grant No. CHE-8806365 from the National Science Foundation.

Registry No. Pt^{4+}, 22541-31-7; Cs_2SiF_6, 16923-87-8; Cs_2GeF_6, 16919-21-4; PtF_6^{2-}, 16871-53-7.